First-principles study on the electronic and optical properties of $Na_{0.5}Bi_{0.5}TiO_3$ lead-free piezoelectric crystal

Min Zeng,[1] Siu Wing Or,[2] and Helen Lai Wa Chan[1,a)]
[1]*Department of Applied Physics, The Hong Kong Polytechnic University, Hung Hom, Kowloon, Hong Kong*
[2]*Department of Electrical Engineering, The Hong Kong Polytechnic University, Hung Hom, Kowloon, Hong Kong*

(Received 8 November 2009; accepted 9 January 2010; published online 22 February 2010)

First-principles calculation is used to study the structural, electronic, and optical properties of $Na_{0.5}Bi_{0.5}TiO_3$ (NBT) lead-free piezoelectric crystal. The band structure calculation reveals that NBT has a direct band gap of 2.1 eV. The calculated imaginary part of dielectric function indicates interband transition mainly from O 2*p* valence bands to Ti 3*d* and Bi 6*p* conduction bands in the low-energy region. The calculated absorption spectrum is in agreement with the available experimental data. Based on the fit of the result of optical abruption spectrum, the optical band gap is estimated to be 3.03 eV. Other optical constants, such as refractive index, extinction coefficient, energy-loss spectrum, and reflectivity are discussed in details. Those found show that NBT has the potential applications in optoelectrics. © *2010 American Institute of Physics*. [doi:10.1063/1.3309407]

I. INTRODUCTION

Sodium bismuth titanate $Na_{0.5}Bi_{0.5}TiO_3$ (NBT) is a ferroelectric complex perovskite-structure compounds with two different ions at the A site of the ABO_3 structure. Since NBT have been discovered by Smolensky *et al.*,[1] it has attracted extensively attention as a promising environmental friendly lead-free ferroelectric material due to its possible applicability to electromechanical actuators, sensor, and transducers.[2] Also the NBT has a very peculiar sequence of phase transitions[3,4] from the cubic ($Pm\bar{3}m$) at the temperature above 813 K, to the tetragonal ($P4bm$) in the range of 783–813 K, and then to the rhombohedral ($R3c$) structure at the temperature below 517 K, which shows unusual dielectric and ferroelectric properties.[3–5] In the ferroelectric phase, the NBT ceramic has a large remanent polarization of $P_r = 38\ \mu C/cm^2$ as well as a large coercive field of $E_c = 73$ kV/cm at room temperature.[5] Regarding these product properties, however, the large coercive field and relatively large conductivity make the NBT ceramic is hard to be poled and its piezoelectric properties are not desirable. Therefore, the most studies has been focused on improving its piezoelectric proprieties by fabricating NBT-based solid solutions, such as $(1-x)(Na_{0.5}Bi_{0.5})TiO_3-xBaTiO_3$,[6,7] and NBT single crystal.[8,9]

Compared with NBT ceramic, NBT single crystal presents good piezoelectric properties and rich optical properties.[5,8–11] Ge *et al.*,[10] reported an optical property of a large-size NBT single crystal fabricated by using top-seeded-solution growth method. Although a NBT single crystal has been fabricated by using different growth methods,[5,8–11] the theoretical study on its electronic structure is seriously limited. There is also disparity between different theoretical calculations. Xu and Ching[12] used first-principles local density calculations to obtain a semiconductor property with a band gap of about 1 eV. On the other hand, Bujakiewicz-Koroska and Natanzon[13] used a generalized gradient approximation (GGA) method to obtain a band gap of about 2 eV. The prediction of the band gap indicates that NBT is a good optical material. However, no theoretical study is done on the investigation of the optical properties. Especially, the physical mechanism concerning optical properties from atom-core level is not clear. Thus, it is necessary to perform a more accurate first-principles calculation to investigate the electronic and optical properties of a NBT crystal. In the present study, the structural, electronic, and optical properties of NBT crystal were studied based on the accurate density function theory calculations.

II. COMPUTATIONAL METHODS

The calculations were performed using an accurate full potential linearized augmented plane-wave method (FP-LAPW), as implemented in WIEN2K code.[14,15] Exchange and correlation effects are used the GGA potential within the Perdew–Burke–Ernzerhof. The muffin-tin radii are 2.37, 2.32, 1.91, and 1.69 a.u. for Na, Bi, Ti, and O atoms, respectively. The plane wave cut-off for the scalar relativistic basic function are $R_{mt}K_{max}=7$ and $l_{max}=12$. Integrations in the reciprocal space were performed with tetrahedron method in a $12\times12\times12$ mesh which represents 292 k-points in the irreducible Brillouin zone (BZ). The ferroelectric phase of NBT belongs to rhombohedral structure with a spacegroup $R3c$ (C_{3v}^6) (disordered Na, Bi in Wyckoff position 2*a*, Ti in 2*a* and O in 6*a*). The fully-relaxed crystal structure (see Table I) is in good agreement with the experimental results.[17]

It is well known that the dielectric function is mainly contributed to electronic interband transitions. The imaginary part $\varepsilon_2(\omega)$ of the dielectric function is calculated from the momentum matrix elements between the occupied and unoccupied wave functions and given by Fermi golden rule, i.e.,[16]

a)Authors to whom correspondence should be addressed. Electronic addresses: apahlcha@inet.polyu.edu.hk and 07900207r@polyu.edu.hk.

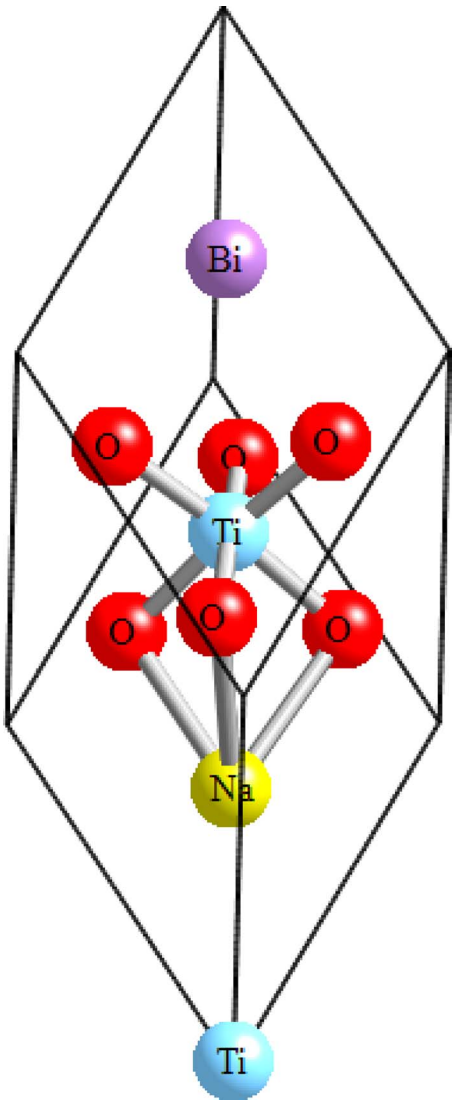

FIG. 1. (Color online) Crystal structure of NBT.

$$\varepsilon_2(\omega) = \frac{4\pi^2}{\Omega\omega^2} \sum_{i\in \mathrm{VB}, j\in \mathrm{CB}} \sum_k w_k |p_{ji}^a|^2 \delta(\varepsilon_{k_j} - \varepsilon_{k_i} - \omega), \quad (1)$$

where Ω is the unit-cell volume and ω is the photon energy, CB and VB denote the conduction band and valence band, respectively, the dipolar transition matrix elements $p_{ij}^a = \langle k_j | P_a | k_i \rangle$ are obtained from the self-consistent band structures within the projector-augmented wave (PAW) formalism. Here, $|k_n\rangle$ is the nth Bloch state wave function with crystal momentum k, and a denotes the Cartesian component. The real part $\varepsilon_1(\omega)$ of dielectric function is evaluated from imaginary part $\varepsilon_2(\omega)$ by the Kramers–Kronig transformation.

$$\varepsilon_1(\omega) = 1 + \frac{2}{\pi} P \int_0^\infty d\omega \frac{\omega' \varepsilon_2(\omega')}{\omega'^2 - \omega^2}, \quad (2)$$

where P is the principle value of the integral. Thus, the complex dielectric function can be expressed as follows:

$$\varepsilon(\omega) = \varepsilon_1(\omega) + i\varepsilon_2(\omega). \quad (3)$$

From the given $\varepsilon(\omega)$, all other linear optical properties can be calculated, e.g., absorption coefficient $a_2(\omega)$ can be obtained by the expression.

$$\alpha_2(\omega) = \sqrt{2}\omega[\sqrt{\varepsilon_1^2(\omega) + j\varepsilon_2^2(\omega)} - \varepsilon_1(\omega)]^{1/2}. \quad (4)$$

TABLE I. Calculated structure parameter for $R3c$ NBT with a=0.557 nm α=59.6832°. The experimental data (Ref. 17) are shown in parentheses with a=0.551 nm and α=59.8028°.

Site	Wyckoff	x	y	z
Na/Bi	2a	0.2699(0.2627)	0.2699(0.2627)	0.2699(0.2627)
Ti	2a	0.0123(0.0063)	0.0123(0.0063)	0.0123(0.0063)
O	6a	0.1814(0.2093)	0.3138(0.2093)	0.7447(0.7473)

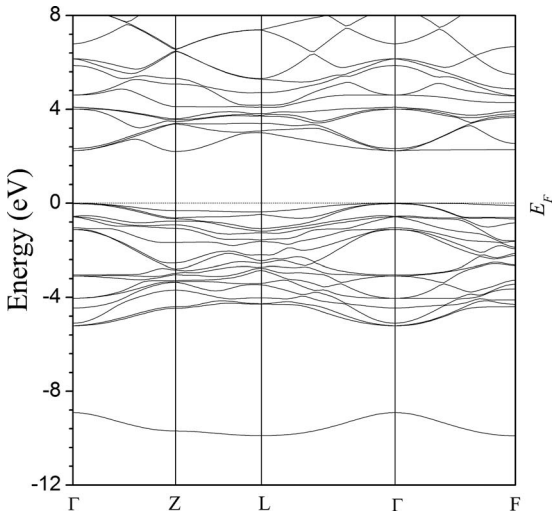

FIG. 2. The calculated band structure of NBT along high-symmetrical directions in the BZ.

III. RESULTS AND DISCUSSIONS

A. Crystal structure and ferroelectric distortion

As shown in Fig. 1, the ferroelectric phase of NBT has a $R3c$ polarized symmetry, which could be distorted from the cubic phase. One is the equal antiphase tilting of neighboring O octahedral about the crystallographic axis [111]. Another is that Bi, Na, Ti, and O atoms are displaced relative to each other along this threefold axis, which gives rise to spontaneous electric polarization along the cubic body diagonal [111] direction. All cations undergo in-phase polar shift, see Table I, implying a strong coupling with O atoms, which is supported by neutron-scattering results.[17,18]

B. Band structure and density of states (DOS)

Figure 2 shows the calculated band structure of NBT along high-symmetric directions in the BZ. It is observed that the top of valence band (VB) and the bottom of conduction band (CB) are both exactly located at highly symmetric Γ point. Thus, a direct band gap is formed and the value is about 2.1 eV, which agrees well with the calculated results in Ref. 13.

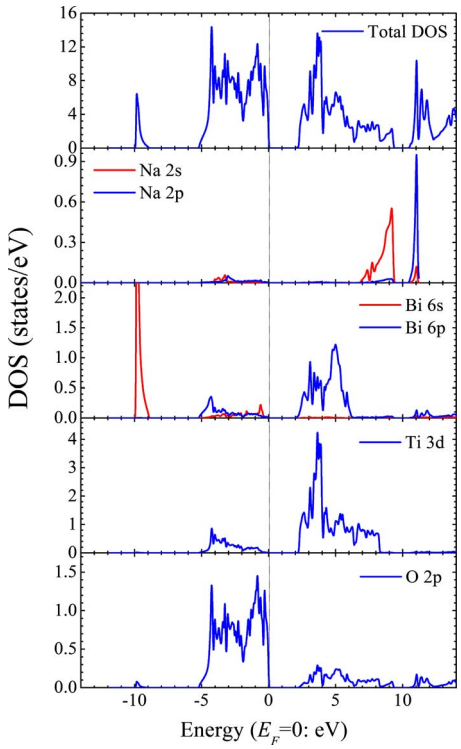

FIG. 3. (Color online) Total and partial DOS of NBT.

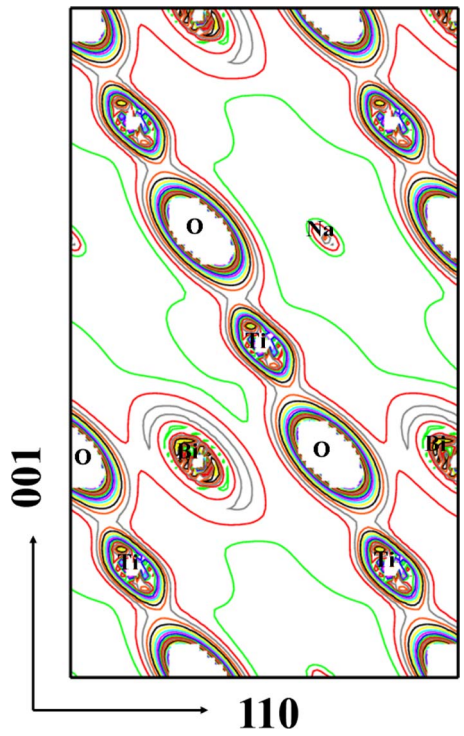

FIG. 4. (Color online) Contour map of the charge density distributions of NBT in the $\langle 1\bar{1}0\rangle$ direction.

Total and partial DOS are given in Fig. 3. A strong peak of O 2*s* states at about −18 eV is omitted from the DOS graph. In the VB, the energy bands at −9.5 eV are mainly from Bi 6*s* states. Above these bands is the band of the O 2*p*, Ti 3*d*, and Bi 6*p* states, which presents a strong hybridization among them. In the CB, the energy bands in the range of 2.1–7.7 eV are mainly dominated by Ti 3*d*, Bi 6*p*, and Na 2*s* states as well as the hybridized O 2*p* states. At high energy bands from 10.5 to 13.5 eV, the strong mixture of Na 2*p* and Bi 6*p* states attributes the energy bands. The corresponding contour map of the charge density distributions of NBT in the $\langle 1\bar{1}0\rangle$ direction is presented in Fig. 4. The strong hybridization effects of Ti–O and Bi–O states are obvious, indicating the driving force of ferroelectricity in such A and/or B-site driven ferroelectric materials. It should be noted that the top in the VB (at Γ) is O 2*p* states and the bottom in the CB (at Γ) is Ti 3*d* and Bi 6*p* states. Thus, the electric properties of NBT as well as optical properties are considered to be determined by the charge-transfer transitions from O 2*p* to Ti 3*d* or Bi 6*p* states.

C. Dielectric and optical properties

The calculated dielectric functions of NBT are displayed in Fig. 5. The imaginary part $\varepsilon_2(\omega)$ of the dielectric function is directly connected with the energy band structure. The first peak A at 4.12 eV corresponds mainly to the transitions from the O 2*p* VB to Ti 3*d* or Bi 6*p* lower-energy CB. This peak is very strong and very much far higher than other peaks. Other peaks as fellows, peaks B (5.12 eV) and C (7.02 eV) are due to the transition from O 2*p* VB to Ti 3*d* or Bi 6*p* high-energy CB. Peak D (11.9 eV) and E (15.3 eV) is ascribed to the transition from O 2*p* VB to Na 2*s* and 2*p* CB. Peak F (20.15 eV) corresponds mainly to the excitation of inner electrons from near O 2*s* semicore VB to CB.

For the $a_2(\omega)$ calculation, we consider only the eigen-absorption and ignore the polarized absorption, which has a minor influence on the $a_2(\omega)$.[19] Figure 6 gives the comparison of the calculated (solid line) and the experimental (symbol line, taken from Ref. 10) optical absorption spectrum $a_2(\omega)$ as a function of photon energy. $a_2(\omega)$ is almost zero in the low-energy region and increases rapidly in the high-energy region. By contrast, the calculated $a_2(\omega)$ is in agreement with the experiment data. The slightly difference is due to using large Gaussian smearing factor, as such broadening

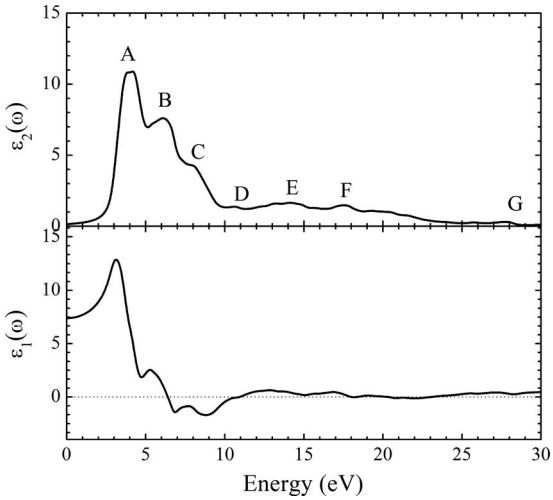

FIG. 5. The calculated (a) imaginary part $\varepsilon_2(\omega)$ and (b) real part $\varepsilon_1(\omega)$ of the dielectric function of the ferroelectric NBT crystal as a function of the photon energy.

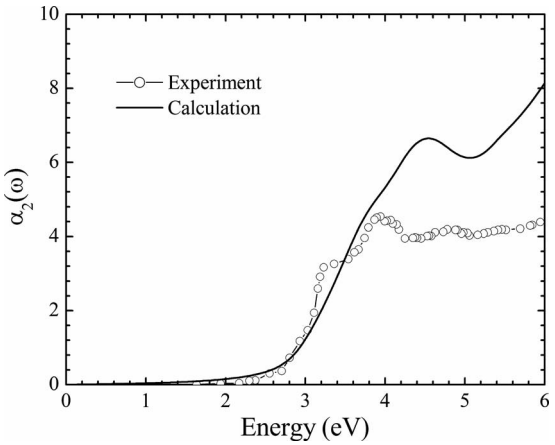

FIG. 6. Comparison of the calculated (solid line) and the experimental (symbol line, taken from Ref. 10) optical absorption spectrum $a_2(\omega)$ as a function of photon energy.

can influence the intensity of the peak.[20] It is well known that the relation between the optical band gap and the absorption coefficient is given by.[21] $\alpha h\upsilon = c(h\upsilon - E_g)^{1/2}$, where h is the planck constant, c is a constant for a direct transition, υ is the frequency of radiation, and α is the optical absorption coefficient. The optical band gap E_g can be obtained from the intercept of $(\alpha h\upsilon)^2$ versus photon energy $(h\upsilon)$. By using the extrapolation, the E_g is estimated to be 3.03 eV in the NBT crystal.

Other optical constant can be also calculated from the complex dielectric function. Figures 7(a)–7(e) display the calculated optical constants of BNT on photon energy dependence of refractive index, extinction coefficient, energy-loss spectrum, and reflectivity, respectively. These parameters are very important to the optical material and related applications.[22] In the range from 0 to 2.0 eV and above 10 eV, the reflectivity [Fig. 7(d)] is lower than 25%, which indicates that NBT is transparent for photons at these ranges.

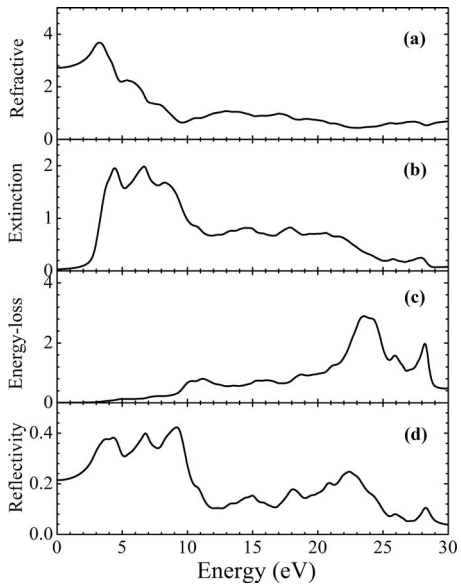

FIG. 7. The calculated optical constants of the ferroelectric NBT crystal (a) refractive index, (b) extinction coefficient, (c) energy-loss spectrum, and (d) reflectivity.

The large extinction coefficient [Fig. 7(b)] is consistent with reflectivity in the range of 2–10 eV. The energy-loss spectrum describes the energy loss of a fast electron traversing the material. The peaks of the loss spectrum [Fig. 7(c)] calculated by our FP-LAPW are at about 23.8 and 28.2 eV, which is associated with the plasma oscillation.[23] This process is associated with transitions from the occupied O 2*s* and Bi 6*s* bands, lying below the VB, to an empty CB. The knowledge of the refractive index of the BNT crystal is necessary for accurate modeling and design of devices. The refractive index [Fig. 7(c)] is large in the low energy range, indicating a high band gap,[22] which is consistent with band structure calculation.

IV. CONCLUSION

In summary, the structural, electronic, and optical properties of free-lead piezoelectric NBT single crystal have been explored by using the FP-LAPW method within the GGA. The fully-relaxed lattice parameters are in good agreement with the experimental data. The electronic structures of NBT revealed that it has a direct band gap of 2.1 eV. The complex dielectric functions, optical constants such as absorption spectrum, refractive index, extinction coefficient, reflectivity, and energy-loss spectrum were calculated and discussed in details. The features of the optical spectra of NBT are mainly determined by the contributions from O 2*p* VBs to Ti 3*d* and Bi 6*p* CBs in the low-energy region. Our studies may pave the way for the application of optelectrics in the NBT.

ACKNOWLEDGMENTS

This work is supported by the Hong Kong Polytechnic University Niche Area Projects (Project Nos. 1-BB95 and 1-BBZ3) and National Natural Science Foundation of China (Grant No. 50862005).

[1] G. A. Smolensky, V. A. Isupov, A. I. Agranovskaya, and N. N. Krainik, Sov. Phys. Solid State **2**, 2651 (1961).
[2] K. Uchino, *Ferroelectric Devices* (Marcel Dekker, New York, 2000).
[3] S. B. Vakhrushev, V. A. Isupov, B. E. Kvyatkovsky, N. M. Okuneva, I. P. Pronin, G. A. Smolensky, and P. P. Syrnikov, Ferroelectrics **63**, 153 (1985).
[4] J. Suchanicz and J. Kwapulin'ski, Ferroelectrics **165**, 249 (1995).
[5] S.-E. Park, S.-J. Chung, and I.-T. Kim, J. Am. Ceram. Soc. **79**, 1290 (1996).
[6] T. Takenaka, K. Maruyama, and K. Sakata, Jpn. J. Appl. Phys., Part 1 **30**, 2236 (1991).
[7] Y. Hiruma, H. Nagata, and T. Takenaka, J. Appl. Phys. **104**, 124106 (2008).
[8] Y. Hosono, K. Harada, and Y. Yamashita, Jpn. J. Appl. Phys., Part 1 **40**, 5722 (2001).
[9] G. Xu, Z. Duan, X. Wang, and D. Yang, J. Cryst. Growth **275**, 113 (2005).
[10] W. Ge *et al.*, J. Alloys Compd. **462**, 256 (2008).
[11] X. Yia, H. Chen, W. Cao, M. Zhao, D. Yang, G. Ma, C. Yang, and J. Han, J. Cryst. Growth **281**, 364 (2005).
[12] Y.-N. Xu and W. Y. Ching, Philos. Mag. B **80**, 1141 (2000).
[13] R. Bujakiewicz-Koroska and Y. Natanzon, Phase Transitions **81**, 1117 (2008).
[14] D. J. Singh, Phys. Rev. B **43**, 6388 (1991).
[15] P. Blaha, K. Schwarz, G. K. H. Madsen, D. Kvasnicka, and J. Luitz, *WIEN2K* (Technical University of Vienna, Austria, 2001).
[16] S. Ju, T.-Y. Cai, and G.-Y. Guo, J. Chem. Phys. **130**, 214708 (2009).
[17] G. O. Jones and P. A. Thomas, Acta Crystallogr. B **58**, 168 (2002).
[18] G. O. Jones and P. A. Thomas, Acta Crystallogr. B **56**, 426 (2000).
[19] C. Persson, R. Ahuja, A. Ferreira da Silva, and B. Johansson, J. Cryst.

Growth **231**, 407 (2001).
[20]H. Wang, Y. Zheng, M.-Q. Cai, H. Huang, and H. L. W. Chan, Solid State Commun. **149**, 641 (2009).
[21]N. Serpone, D. Lawless, and R. Khairutdinov, J. Phys. Chem. **99**, 16646 (1995).
[22]X. D. Zhang, M. L. Guo, W. X. Li, and C. L. Liu, J. Appl. Phys. **103**, 063721 (2008).
[23]M.-Q. Cai, Z. Yin, and M.-S. Zhang, Appl. Phys. Lett. **83**, 2805 (2003).